Acta Pharmacologica Sinica

www.nature.com/aps

ARTICLE

Triptolide protects against white matter injury induced by chronic cerebral hypoperfusion in mice

Yu-shan Wan[1], Yi You[1], Qian-yun Ding[1,2], Yi-xin Xu[1], Han Chen[1], Rong-rong Wang[3], Yu-wen Huang[1], Zhong Chen[1,2], Wei-wei Hu[1] and Lei Jiang[1]

White matter injury is the major pathological alteration of subcortical ischemic vascular dementia (SIVD) caused by chronic cerebral hypoperfusion. It is characterized by progressive demyelination, apoptosis of oligodendrocytes and microglial activation, which leads to impairment of cognitive function. Triptolide exhibits a variety of pharmacological activities including anti-inflammation, immunosuppression and antitumor, etc. In this study, we investigated the effects of triptolide on white matter injury and cognitive impairments in mice with chronic cerebral hypoperfusion induced by the right unilateral common carotid artery occlusion (rUCCAO). We showed that triptolide administration alleviated the demyelination, axonal injury, and oligodendrocyte loss in the mice. Triptolide also improved cognitive function in novel object recognition test and Morris water maze test. In primary oligodendrocytes following oxygen-glucose deprivation (OGD), application of triptolide (0.001−0.1 nM) exerted concentration-dependent protection. We revealed that the protective effect of triptolide resulted from its inhibition of oligodendrocyte apoptosis via increasing the phosphorylation of the Src/Akt/GSK3β pathway. Moreover, triptolide suppressed microglial activation and proinflammatory cytokines expression after chronic cerebral hypoperfusion in mice and in BV2 microglial cells following OGD, which also contributing to its alleviation of white matter injury. Importantly, mice received triptolide at the dose of 20 μg·kg^{-1}·d^{-1} did not show hepatotoxicity and nephrotoxicity even after chronic treatment. Thus, our results highlight that triptolide alleviates whiter matter injury induced by chronic cerebral hypoperfusion through direct protection against oligodendrocyte apoptosis and indirect protection by inhibition of microglial inflammation. Triptolide may have novel indication in clinic such as the treatment of chronic cerebral hypoperfusion-induced SIVD.

Keywords: triptolide; chronic cerebral hypoperfusion; white matter injury; microglial activation; right unilateral common carotid artery occlusion (rUCCAO); oligodendrocyte

Acta Pharmacologica Sinica (2022) 43:15–25; https://doi.org/10.1038/s41401-021-00637-0

INTRODUCTION

Subcortical ischemic vascular dementia (SIVD), a common subtype of ischemic dementia, is often caused by chronic cerebral hypoperfusion. Clinically, SIVD leads to impairment of language, emotion, and especially cognitive function. The major pathological change in SIVD is white matter injury, which is characterized by progressive demyelination, oligodendrocyte apoptosis and microglial activation [1]. Currently, there are no effective treatments for SIVD apart from improving cerebral circulation and metabolism. Therefore, there is an urgent need for novel agents to alleviate white matter injury by suppressing oligodendrocyte apoptosis or microglial activation.

Triptolide is extracted from *Tripterygium wilfordii*, which is a traditional Chinese medicine and has been used to treat rheumatism and immune diseases in the clinic. Triptolide exhibits multiple pharmacological functions, including potent immunomodulatory and anti-inflammatory activities, to treat autoimmune diseases as well as antitumor effects to treat a variety of cancers [2, 3]. However, its clinical application has been limited due to its potential multiorgan toxicity, especially its extremely severe toxic effects when taken at high doses [4, 5]. In recent years, an increasing number of studies have focused on the neuroprotective effects of relatively low doses of triptolide against traumatic brain injury, ischemic stroke, neuropathic pain and experimental autoimmune encephalomyelitis [6–10]. Triptolide easily penetrates the blood-brain barrier because of its small molecular size and high lipophilicity [11]. Its protective effects largely derive from its inhibition of neuronal apoptosis, microglial activation and proinflammatory cytokine release [12, 13]. Triptolide inhibited TNF-α, IL-1β and NO production in primary microglial cultures [14, 15]. However, the effect of triptolide on white matter injury after chronic cerebral hypoperfusion has not yet been investigated.

To determine whether triptolide has neuroprotective and anti-inflammatory effects against SIVD, we generated a reliable model of right unilateral common carotid artery occlusion (rUCCAO), which induces white matter injury and cognitive impairment

[1]Department of Pharmacology and Department of Pharmacy of the Second Affiliated Hospital, NHC and CAMS Key Laboratory of Medical Neurobiology, Department of Anatomy, School of Basic Medical Science, Zhejiang University School of Medicine, Hangzhou 310058, China; [2]College of Pharmaceutical Sciences, Zhejiang Chinese Medical University, Hangzhou 310053, China and [3]Department of Clinical Pharmacy, The First Affiliated Hospital, College of Medicine, Zhejiang University, Hangzhou 310003, China
Correspondence: Wei-wei Hu (huww@zju.edu.cn) or Lei Jiang (jiang_lei@zju.edu.cn)
These authors contributed equally: Yu-shan Wan, Yi You, Qian-yun Ding

Received: 8 September 2020 Accepted: 3 March 2021
Published online: 6 April 2021

through chronic cerebral hypoperfusion, as detected by laser Doppler flowmetry [16–19]. In addition, this mouse model shows low mortality and no apparent neuronal loss in the hippocampus [18]. In previous studies, the neuroprotective dose of triptolide ranged from 5 to 100 μg·kg^{-1}·d^{-1} [20–22]. To avoid potential toxicity from a high dose of triptolide, we chose to use low doses of triptolide (5 and 20 μg·kg^{-1}·d^{-1}) for the present experiments. Furthermore, primary cultured oligodendrocytes and microglia as well as the Oli-neu and BV2 cell lines were used for in vitro experiments. We demonstrated that treatment with triptolide alleviated white matter injury and reduced cognitive impairment induced by chronic cerebral hypoperfusion. These effects were due to its direct inhibition of oligodendrocyte apoptosis through the Src/Akt/GSK3β pathway and its suppression of microglial activation.

MATERIALS AND METHODS

Animals and treatments

All experiments using animals were performed in accordance with the National Institutes of Health Guide for the Care and Use of Laboratory Animals. Eight-week-old wild-type (WT, C57BL/6 strain) male mice were randomly divided into the sham group, the rUCCAO group, the rUCCAO + triptolide 5 μg·kg^{-1}·d^{-1} group and the rUCCAO + triptolide 20 μg·kg^{-1}·d^{-1} group. All the groups survived for 4 weeks after rUCCAO for use in behavioral experiments, histochemical examination and biochemical assays. Histochemical examination was also performed at 7 days after rUCCAO.

For the rUCCAO operation, mice were administered sodium pentobarbital (60 mg/kg) for anesthesia by intraperitoneal injection and fixed on the operation table. After disinfection with 75% alcohol, the middle of the neck was cut open. The right common carotid artery was isolated from the vagus nerve and double-ligated proximal and distal to the heart with 6-0 silk. The skin was sutured with 6-0 silk and disinfected with iodine. Sham-operated mice were subjected to the same procedure but without carotid ligation. During recovery from anesthesia, the mice were kept in a heated cage to maintain body temperature.

Triptolide, which is a white crystalline material, was purchased from Yuanye Biology (Shanghai, China) at 98% purity estimated by high-performance liquid chromatography. Triptolide was dissolved in dimethylsulfoxide and diluted to the appropriate concentrations in saline. Mice were administered saline or triptolide (5 or 20 μg/kg) by intraperitoneal injection 30 min after rUCCAO and were injected daily until the mice were killed.

Mice were subjected to the novel object recognition test and Morris water maze test from D21 to D27 after rUCCAO. On D28, the mice were sacrificed, and brain tissues were removed for immunostaining, Western blot and ELISAs. Serum was obtained from mice on D28, and serum biochemical indicators such as aspartate aminotransferase (AST), alanine aminotransferase (ALT), total albumin (ALB), blood urea nitrogen (BUN) and creatinine were analyzed by kits purchased from Nanjing Jiancheng Bioengineering Institute (Nanjing, China).

Novel object recognition test

An opaque plexiglass box (45 cm × 45 cm × 45 cm) and two different kinds of objects were used in the test. On the first day, mice were allowed to freely explore the empty box for 10 min. The next day, the mice were exposed to the familiar box with two identical objects presented on two opposite sides of the box and allowed to freely explore for 10 min. After a 30-min interval, one of the objects was replaced with a new object, and the mice were allowed to freely explore for 3 min. Directing the nose toward the object at a distance <1 cm from the object and/or touching it with the nose was recorded as exploration. Time during which the mouse climbed to the top of the object or remained on top of the object was not included. After each trial, the glass box and objects were carefully cleaned with 75% alcohol to eliminate olfactory stimuli. The exploration time spent on each of the familiar (F) objects and the new (N) object was recorded manually in a blind manner. For intergroup comparison, the discrimination index percentage was calculated by the following equation: discrimination index percentage = ((N − F)/(N + F))*100%.

Morris water maze test

For this test, a circular pool (diameter, 150 cm) was filled with water (21 ± 1.5 °C) and painted white. The pool was divided into four quadrants (NE, NW, SW, and SE) by two hypothetical vertical lines through the center of the surface. The round escape platform (diameter,10 cm) was submerged 1.5 cm below the water surface and placed in the center of one quadrant of the pool. Several distal cues were provided around the tank to orient the mouse as it navigated within the pool, and these cues remained in the same position throughout the training and testing periods. White pigment was added to the water to prevent the mice from seeing the platform directly. Our experiment included 4 trials per day on the first 4 days (the training period) and 1 trial on the last day (the testing period). During the training period, each mouse was placed randomly in one of four quadrants in the water, and the escape latency was defined as the time it took for a mouse to find the platform and stay on it for 5 s within 60 s. If the mouse did not find the platform within 60 s, it was gently guided to the platform and allowed to stay for 10 s. The average escape latency was calculated for each day. During the testing period, the platform was removed, and the mice were allowed to freely explore the pool for 60 s. The time spent in the target quadrant was recorded.

Western blot assay

The samples were lysed in RIPA buffer containing 20 mM Tris-HCL (pH 7.5), 1.5 M NaCl, 1% Triton X-100, 0.5% sodium deoxycholate, 0.1% SDS, 1 mM EDTA, 20 mM NaF and protease inhibitors (Roche, Switzerland). Supernatants were collected after centrifugation at 12,000 rpm for 20 min at 4 °C. The protein concentration in the supernatant was determined using the BCA Assay Kit (Thermo, USA). An aliquot of 40 μg total protein from each sample was loaded onto 10% SDS-PAGE gels and transferred to a nitrocellulose membrane that was then incubated with primary antibodies against MBP (1:1000; Millipore, USA), p-Src (Tyr416)(1:1000; Cell Signaling Technology, USA), Src (1:1000; Cell Signaling Technology), p-Akt (1:1000, Abcam, UK), Akt (1:1000, Abcam), p-GSK3β (Ser9) (1:1000, Abcam), GSK3β (1:1000, Abcam), Bcl-2 (1:1000, Abcam), Bax (1:1000, Abcam), cleaved-caspase3 (1:1000, Abcam), p-Erk1/2 (1:1000; Cell Signaling Technology), Erk1/2 (1:1000; Cell Signaling Technology), p-p38 (1:1000; Cell Signaling Technology), p38 (1:1000; Cell Signaling Technology), p-JNK (1:1000; Cell Signaling Technology), JNK (1:1000; Cell Signaling Technology), or GAPDH (1:5000; Kang-chen, China) overnight at 4 °C. The membranes were washed three times with TBST buffer and incubated with secondary antibodies against rat, rabbit or mouse IgG (1:3000; Multi Sciences, China) for 2 h at room temperature. The membranes were visualized using an enhanced chemiluminescence detection system (Tanon, China).

Immunofluorescent staining

Mice were transcardially perfused with a solution containing 0.9% NaCl followed by 4% paraformaldehyde (PFA) in 0.1 M PBS (pH 7.4). Frozen coronal brain sections (25 μm thick) were obtained using a cryostat (CryoStar NX50, Thermo Fisher, USA). After blocking with 5% donkey serum, the sections were incubated over night at 4 °C with the following primary antibodies: rabbit anti-Olig2 (1:500, Millipore), rat anti-MBP (1:400; Millipore), anti-NF200 (1:100; Abcam), mouse anti-CC-1 (1:400; Abcam) or rabbit anti-Iba1 (1:1000; Wako, Japan) antibody. The sections were washed three times with PBS buffer and incubated with secondary antibodies including AlexaFluor-488- and AlexaFluor-594-conjugated

secondary antibodies to rat, rabbit or mouse IgG (1:400; Jackson ImmunoResearch Laboratories, USA) for 2 h at room temperature. Apoptotic cells were identified using a terminal deoxynucleotidyl transferase dUTP nick end labeling (TUNEL) assay (Yeasen, China) according to the manufacturer's protocol before incubation with primary antibodies. The sections were observed under a fluorescence microscope (Olympus, Japan). Fluorescence intensity measurement and cell counting were performed using ImageJ software (NIH, USA) from images of the ipsilateral corpus callosum at a similar coronal position of each animal.

IL-6 and TNF-α expression by ELISA

The samples were dissected from the corpus callosum ipsilateral to the rUCCAO and homogenized in a buffer containing protease inhibitors (Roche). Supernatants were collected after centrifugation at 12,000 r/min for 10 min at 4 °C. The concentrations of IL-6 and TNF-α were detected using purified biotinylated antibodies in ELISA kits (Boster, China) according to the manufacturer's instructions and were expressed as pg/mg wet weight. The ELISA plates were read using a spectrophotometer (Biotek, USA).

Primary cortical oligodendrocyte and microglia culture

Purified oligodendrocytes were isolated by the shake-off method as previously described with some modifications [19, 23]. Mixed cortical glial cell cultures were generated from newborn (P0) SD rats and maintained in Dulbecco's modified Eagle's medium (DMEM, Invitrogen, USA) with 20% fetal bovine serum (FBS, Biological Industries, Israel) for 6–10 days at 37 °C under 5% CO_2. The medium was changed every three days. The culture flasks were shaken horizontally by hand a dozen times for microglial collection and shaken at 200 rpm for 1 h followed by additional shaking at 250 r/min for 14–16 h with fresh medium at 37 °C for oligodendrocyte precursor cell (OPC) collection. The OPC suspension was seeded onto poly-*L*-lysine-coated dishes or coverslips in neurobasal medium supplemented with 2% B27 (Invitrogen) and 3,3′,5-triiodo-*L*-thyronine (T3, 40 ng/mL; Sigma-Aldrich, USA) and ciliary neurotrophic factor (CNTF, 10 ng/mL; Sigma-Aldrich), which were added to allow their differentiation into mature oligodendrocytes. The purity of oligodendrocytes was confirmed by immunocytochemical staining of the oligodendrocyte marker Olig2, which stained 90.6% ± 4.2% of the total cells. Microglial cells were cultured in MEM (Gibco, New Zealand) with 3% FBS and matured after 6–10 days. In the coculture system, mature microglial cells were seeded onto the upper chamber, and mature oligodendrocytes were seeded onto poly-*L*-lysine-coated coverslips in the lower chamber of a Transwell plate in neurobasal medium supplemented with 2% B27.

Cell line culture

The mouse microglial cell line BV2 was provided by Prof. Er-qing Wei of Zhejiang University. As reported before [24], the BV2 cells were cultured in high-glucose DMEM supplemented with 10% FBS at 37 °C with 95% O_2 and 5% CO_2. The culture medium was changed every 2 days.

Dr. Qinjie Weng (Zhejiang University) kindly supplied the immortalized mouse oligodendrocyte cell line (Oli-neu) with permission from Dr. Q. Richard Lu (University of Cincinnati, USA). Oli-neu cells were cultured in DMEM with 5% FBS, 2% B27, 1% horse serum (Gibco, New Zealand) and 1% N_2 (Invitrogen) at 37 °C with 95% O_2 and 5% CO_2. The culture medium was changed every 2 days.

Oxygen-glucose deprivation (OGD) and treatments

The cells were cultured on dishes or plates, and then the medium was replaced with O_2- and glucose-free DMEM, and the cells were immediately placed in a sealed chamber (Billups-Rothenburg, USA) loaded with mixed gas containing 5% CO_2 and 95% N_2 for 5 min. The cells were kept in the chamber for 2 h. Different concentrations of triptolide (0.001, 0.01, and 0.1 nM) were added to the cells for 24 h during reperfusion or to cells without OGD exposure. The control group was cultured in DMEM with glucose for 2 h at 37 °C with 95% O_2 and 5% CO_2. Cells were evaluated by immunohistochemistry, double-staining with-Hoechst 33342 and PI, LDH release assays and Western blot analysis of apoptosis-related proteins.

To study whether the Src/Akt/GSK3β signaling cascade is involved in the action of triptolide, cells were administered triptolide (0.001, 0.01, and 0.1 nM) for 1 h during reperfusion, and then p-Src, Src, p-Akt, Akt, p-GSK3β and GSK3β expression was analyzed by Western blotting. Alternatively, cells were treated with the Src inhibitor PP2 (10 μM; Sigma-Aldrich, USA) or the AKT inhibitor MK2206 (2 μM; Sigma-Aldrich, USA) immediately after reperfusion followed by triptolide (0.1 nM) 1 h later. The expression of p-Src and p-Akt was analyzed 2 h after reperfusion, and cleaved-Caspase-3 (c-Caspase-3) expression was analyzed 24 h after reperfusion.

Hoechst/PI staining

Hoechst 33342/PI staining was performed according to the manufacturer's instructions (Nanjing Jiancheng Bioengineering Institute, China). Briefly, Hoechst 33342 (10 μg/mL) was added to the culture medium for 10 min at 37 °C, and then the cells were incubated with PI (5 μg/mL) for 10 min at 4 °C. After three washes with PBS, the cells were fixed with 4% PFA for 15 min at room temperature. The cells were observed under a fluorescence microscope (Olympus, Japan). The numbers of cells stained with Hoechst 33342 and PI were counted, and the percentages of PI-positive cells among the total Hoechst 33342-stained cells were calculated as an indicator of cell death.

LDH release test

LDH release was measured according to the manufacturer's instructions (Nanjing Jiancheng Bioengineering Institute). LDH release was read at 450 nm using a spectrophotometer (Biotek, USA) and was calculated as the percentage of LDH release.

Statistical analysis

Data were presented as the mean ± standard error of the mean. All data from experiments represented at least three independent experiments. Statistical comparisons among three or more groups were performed by one-way analysis of variance (ANOVA) with Tukey's post hoc test. Escape latency in the Morris water maze test was analyzed by two-way ANOVA with Tukey's post hoc test. For all analyses, the tests were two-sided, and $P < 0.05$ was considered significant. GraphPad Prism 7 software was used for all analyses.

RESULTS

Triptolide alleviated white matter injury induced by chronic cerebral hypoperfusion

We first aimed to determine the effects of triptolide on white matter injury following chronic cerebral hypoperfusion induced by rUCCAO [16, 19]. In this SIVD model, cerebral blood flow measured by a laser Doppler flowmetry probe was significantly decreased compared with that in sham-operated mice (Supplementary Fig. 1). White matter injury in the corpus callosum and hippocampus was evaluated by immunostaining or Western blotting for myelin basic protein (MBP), which is a major component of myelin in the central nervous system. The results showed that MBP expression in the corpus callosum and hippocampus was significantly reduced at 28 days after surgery, indicating demyelination after chronic cerebral hypoperfusion. Triptolide treatment rescued MBP expression at a dosage of 20 $\mu g \cdot kg^{-1} \cdot d^{-1}$, and triptolide treatment at 5 $\mu g \cdot kg^{-1} \cdot d^{-1}$ also increased MBP expression, as shown by immunostaining of the corpus callosum (Fig. 1a–e). To determine whether increased myelin contributed to the rescue of axonal injury, we analyzed the

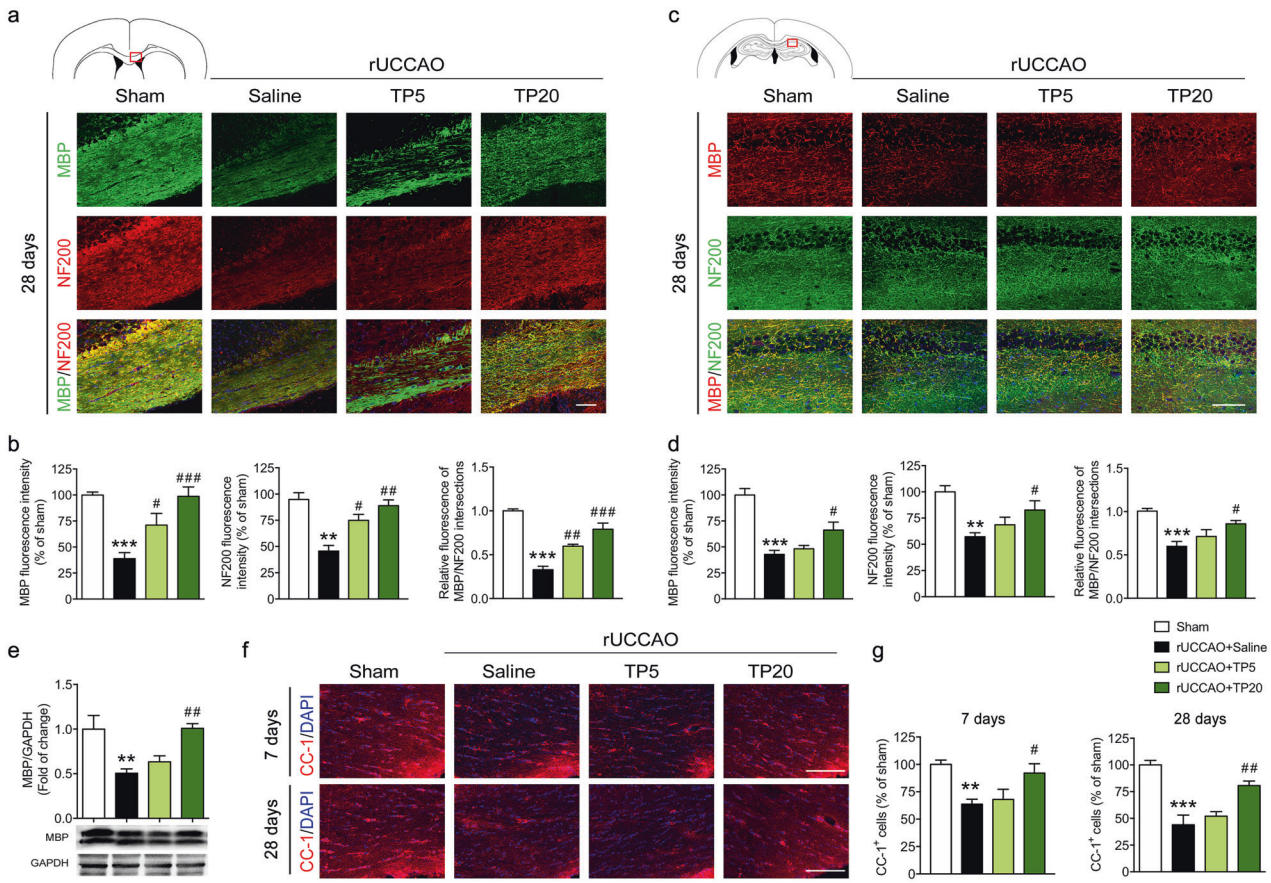

Fig. 1 Triptolide alleviated white matter injury induced by chronic cerebral hypoperfusion. a, **b** Immunohistochemical visualization and quantification of MBP and NF200 and colocalization of NF200 and MBP in the corpus callosum (red outlined rectangle in the schematic diagram) at 28 d after right unilateral common carotid artery occlusion (rUCCAO) in mice administered triptolide at a dosage of 5 μg·kg^{-1}·d^{-1} (TP5) or 20 μg·kg^{-1}·d^{-1} (TP20). **c**, **d** Immunohistochemical visualization and quantification of MBP and NF200 and colocalization of NF200 and MBP in the hippocampus (red outlined rectangle in the schematic diagram) at 28 d after rUCCAO in mice administered TP5 or TP20. **e** Western blot analysis of MBP expression in the corpus callosum at 28 d after rUCCAO. **f**, **g** Immunohistochemical visualization and quantification of CC-1$^+$ oligodendrocyte numbers at 7 d and 28 d after rUCCAO in mice administered TP5 or TP20. Scale bars, 100 μm. $n = 3$–5 mice per group from at least three independent experiments. $^{**}P < 0.01$, $^{***}P < 0.001$ *vs*. the sham group; $^{\#}P < 0.05$, $^{\#\#}P < 0.01$, $^{\#\#\#}P < 0.001$ *vs*. the rUCCAO + saline group.

expression of the neurofilament marker NF200 and its immunofluorescent colocalization with MBP in the corpus callosum and hippocampus. The results showed that treatment with triptolide significantly enhanced both NF200 expression and its localization with MBP at 28 d after surgery (Fig. 1a–d), suggesting reduced myelin and axon injury.

The increase in myelin could result from the alleviation of mature oligodendrocyte damage or remyelination, which takes a long time due to the regeneration of oligodendrocytes. Therefore, we labeled the mature oligodendrocyte marker CC-1 in the white matter at early (7 days) and late stages (28 days) after rUCCAO. We found that the number of CC-1$^+$ oligodendrocytes was decreased at 28 days after rUCCAO surgery, while treatment with triptolide (20 μg·kg^{-1}·d^{-1}) significantly increased the number of CC-1$^+$ mature oligodendrocytes in white matter. Furthermore, we found that triptolide at a dosage of 20 μg·kg^{-1}·d^{-1} also reversed oligodendrocyte loss at 7 d after rUCCAO (Fig. 1f, g). These observations suggested that treatment with triptolide alleviated oligodendrocyte loss to prevent demyelination and axonal injury following chronic cerebral hypoperfusion.

Triptolide alleviated cognitive impairment induced by chronic cerebral hypoperfusion

Since the white matter corpus callosum is associated with cognitive behaviors such as nonspatial memory and spatial memory, we performed novel object recognition tests and Morris water maze tests in mice. In the novel object recognition test, mice showed a significant reduction in discriminative ability after rUCCAO, and triptolide administered at a dosage of 20 μg·kg^{-1}·d^{-1} for the entire duration after rUCCAO markedly increased the discrimination index (Fig. 2a, b). In the Morris water maze tests, the mice exhibited a markedly prolonged escape latency in training trials and a decreased duration in the target quadrant in probing trials after rUCCAO, revealing spatial memory impairments. When triptolide was administered at 20 μg·kg^{-1}·d^{-1}, the escape latencies in the training trials were substantially shortened, and the duration in the target quadrant was prolonged in the probing trials (Fig. 2c–e). The average swim speed showed no differences among all groups (Fig. 2f). These observations revealed that administration of triptolide reduced cognitive impairment following chronic cerebral hypoperfusion.

Triptolide inhibited the apoptosis of oligodendrocytes induced by OGD in vitro

To clarify whether the protective effect of triptolide is due to its direct effect on oligodendrocytes, primary cultured oligodendrocyte cells were subjected to OGD for 2 h and treated with triptolide at three concentrations (0.001, 0.01 and 0.1 nM) for 24 h during reperfusion, which is a common in vitro model to study white matter damage induced by cerebral hypoperfusion [25, 26].

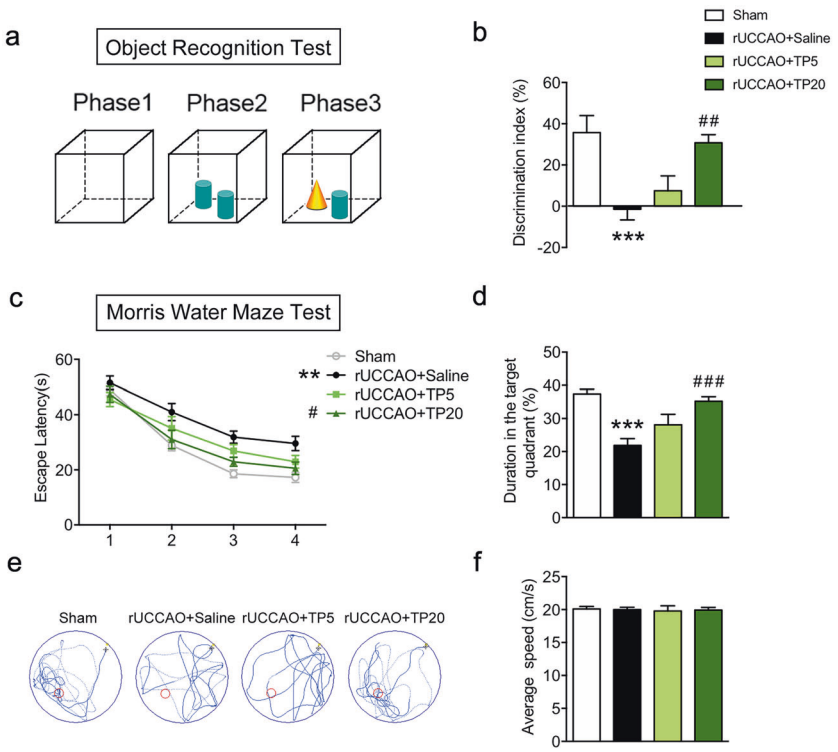

Fig. 2 Triptolide alleviated cognitive impairment induced by chronic cerebral hypoperfusion. Cognitive behavior was evaluated by the discrimination index in the object recognition test (**a**, **b**) and by the Morris water maze test (**c**–**f**) from 21 d to 27 d after rUCCAO in mice administered with triptolide at doses of 5 μg·kg^{-1}·d^{-1} (TP5) or 20 μg·kg^{-1}·d^{-1} (TP20). **c** Latency to reach the platform during the acquisition trials. **d** Searching time in the target quadrant in the probe trial. **e** Diagram of swimming paths in the probe trial. **f** Average speed in the probe trial. $n = 10$–12 mice per group from at least three independent behavior experiments. $^{***}P < 0.001$ *vs*. the sham group; $^{\#\#}P < 0.01$, $^{\#\#\#}P < 0.001$ *vs*. the rUCCAO + saline group.

The number of MBP$^+$ mature oligodendrocytes observed in the immunocytochemistry analysis was decreased after OGD exposure and reperfusion, while triptolide showed a concentration-dependent protective effect (Fig. 3a, b). To verify these results, the effect of triptolide on mature oligodendrocyte viability was assessed by double fluorescent staining with Hoechst 33342 and PI. The results showed that the percentage of injured cells stained with PI out of the total number of cells stained with Hoechst 33342 was markedly decreased in mature oligodendrocytes treated with triptolide after OGD (Fig. 3a, c). Cell damage was also evaluated by lactate dehydrogenase (LDH)-release assay. LDH release was significantly increased after OGD, but this effect was reversed by treatment with 0.1 nM triptolide (Fig. 3d). To verify the effect of triptolide on mature oligodendrocyte apoptosis, TUNEL staining was carried out, and the number of CC-1 and TUNEL double-positive cells was analyzed. The results showed that OGD significantly increased the number of apoptotic mature oligodendrocytes, whereas treatment with triptolide inhibited cell apoptosis (Fig. 3e, f). Furthermore, the expression of apoptosis-related proteins was evaluated in the Oli-neu oligodendrocyte cell line. The protein levels of the antiapoptotic protein Bcl-2 were significantly decreased after 2 h of OGD exposure, whereas the levels of the apoptotic proteins cleaved-Caspase-3 and Bax were increased. After treatment with different concentrations of triptolide, the levels of Bcl-2 were significantly elevated compared with those after OGD treatment alone. In addition, the levels of cleaved-Caspase-3 and Bax were decreased in the triptolide treatment groups compared with the OGD group (Fig. 3g–i). Overall, these results suggested that triptolide exerted a protective effect against OGD-induced oligodendrocyte damage by inhibiting apoptosis in vitro.

Triptolide suppressed apoptosis through the Src/Akt/GSK3β signaling pathway

It has been reported that triptolide affects tumor cell proliferation and apoptosis by regulating the Akt and MAPK signaling pathways [27–29]. We thus determined whether the Akt or MAPK pathway was involved in the effects of triptolide on oligodendrocyte apoptosis by measuring the total protein expression and phosphorylation of Akts and MAPKs, including extracellular signal-regulated kinase 1/2 (ERK1/2), c-Jun N-terminal kinase (JNK), and p38 protein kinase. In oligodendrocytes, OGD decreased the phosphorylation of Akt but had no effect on the total protein level of Akt. The phosphorylation of Akt was increased by treatment with different concentrations of triptolide during OGD (Fig. 4a, b). OGD elevated the expression of phospho-ERK1/2, phospho-JNK and phospho-p38 in oligodendrocytes; however, treatment with triptolide had no effect on the increased levels of phosphorylated MAPKs in oligodendrocytes (Supplementary Fig. 2).

To further investigate the mechanism underlying the triptolide-mediated regulation of oligodendrocyte apoptosis, we searched for other upstream and downstream molecules of Akt. Several studies have shown that the Src/Akt/GSK3β signaling pathway is involved in the apoptosis of oligodendrocytes and Schwann cells [30–32]. Therefore, we measured the levels of total and phosphorylated Src and GSK3β. The results showed that OGD had no effect on total Src or GSK3β in oligodendrocytes but decreased the levels of phospho-Src (Tyr416) and phospho-GSK3β (Ser9). After treatment with triptolide, the phosphorylation of Src and GSK3β was elevated (Fig. 4a, c, d). In addition, the levels of the apoptosis protein cleaved-Caspase-3 in the corpus callosum were increased after rUCCAO, and triptolide treatment completely

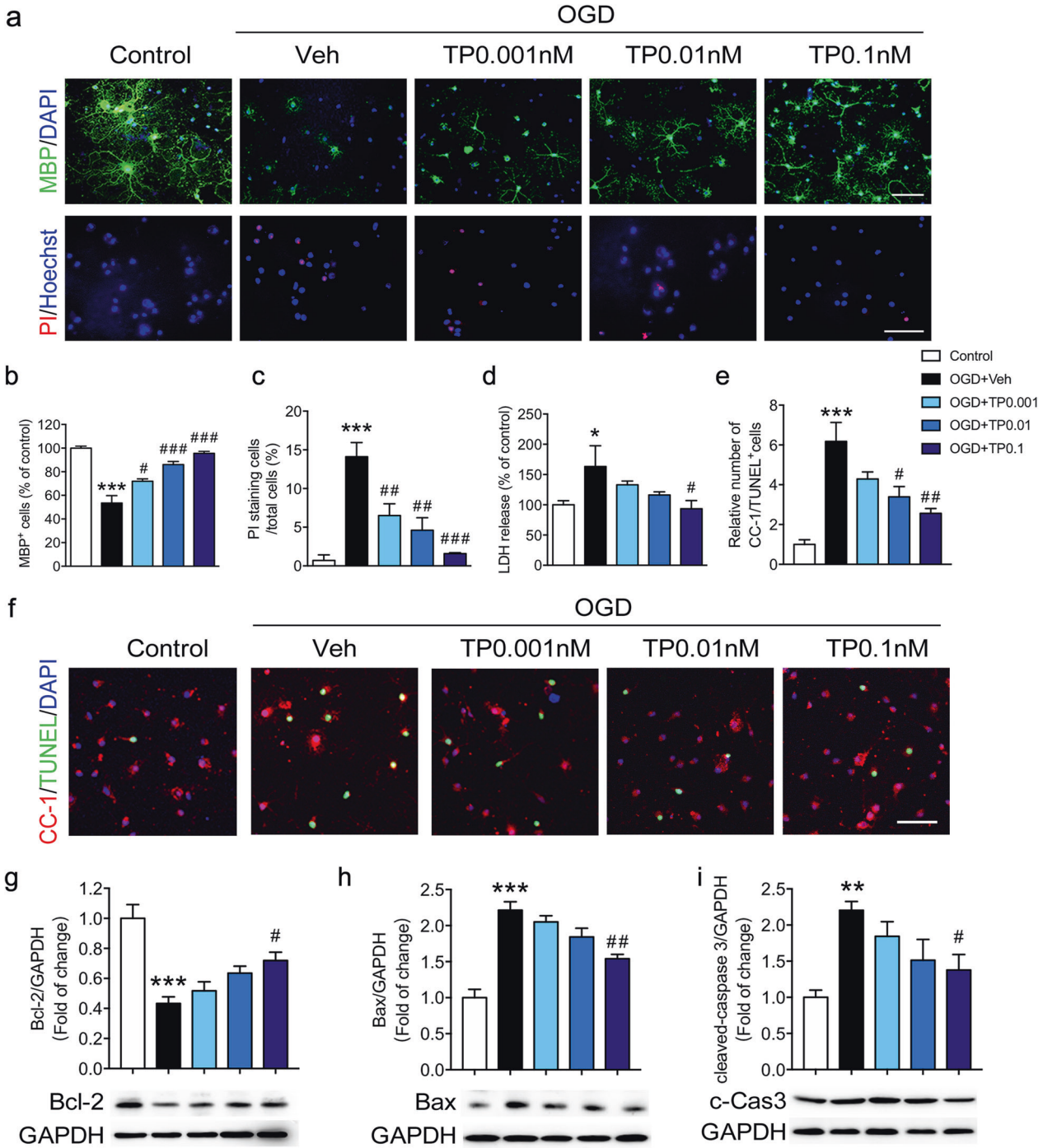

Fig. 3 Triptolide inhibited the apoptosis of oligodendrocytes induced by OGD. Primary cultured mature oligodendrocytes were subjected to OGD for 2 h and administered with triptolide at concentrations of 0.001, 0.01, and 0.1 nM for 24 h during reperfusion. **a**, **b** Immunocytochemical visualization and quantification of the numbers of MBP^+ mature oligodendrocytes after OGD/reperfusion. **a**, **c** Cell death was determined by double-staining with Hoechst 33342 (blue) and propidium iodide (PI, red) in oligodendrocytes after OGD/reperfusion. Scale bars, 50 μm. **d** Cell damage was evaluated by lactate dehydrogenase (LDH) release assays after OGD/reperfusion. **e**, **f** Immunocytochemical visualization and quantification of the numbers of CC-1 and TUNEL double-positive mature oligodendrocytes after OGD/reperfusion. Western blot analysis of the expression of apoptosis-related proteins, including Bcl-2 (**g**), Bax (**h**) and cleaved-Caspase-3 (c-Cas3, **i**), in oligodendrocytes after OGD/reperfusion. $n = 3$–5 from at least three independent experiments. $^*P < 0.05$, $^{**}P < 0.01$, $^{***}P < 0.001$ vs. the control group; $^{\#}P < 0.05$, $^{\#\#}P < 0.01$, $^{\#\#\#}P < 0.001$ vs. the OGD + vehicle (Veh) group.

reversed cleaved-Caspase-3 expression at doses of 5 and 20 $\mu g \cdot kg^{-1} \cdot d^{-1}$ (Supplementary Fig. 3a). Moreover, triptolide treatment also reversed the decrease in phosphorylation of Src and Akt after rUCCAO (Supplementary Fig. 3b–d). To further confirm whether the Src/Akt/GSK3β signaling cascade is involved in the inhibition of oligodendrocyte apoptosis by triptolide, the Src inhibitor PP2 and the Akt inhibitor MK2206 were employed (Fig. 4e–h). We found that the Src inhibitor PP2 reversed the increase in phosphorylation of Src and Akt induced by triptolide following OGD. The Akt inhibitor MK2206 reversed the increase in

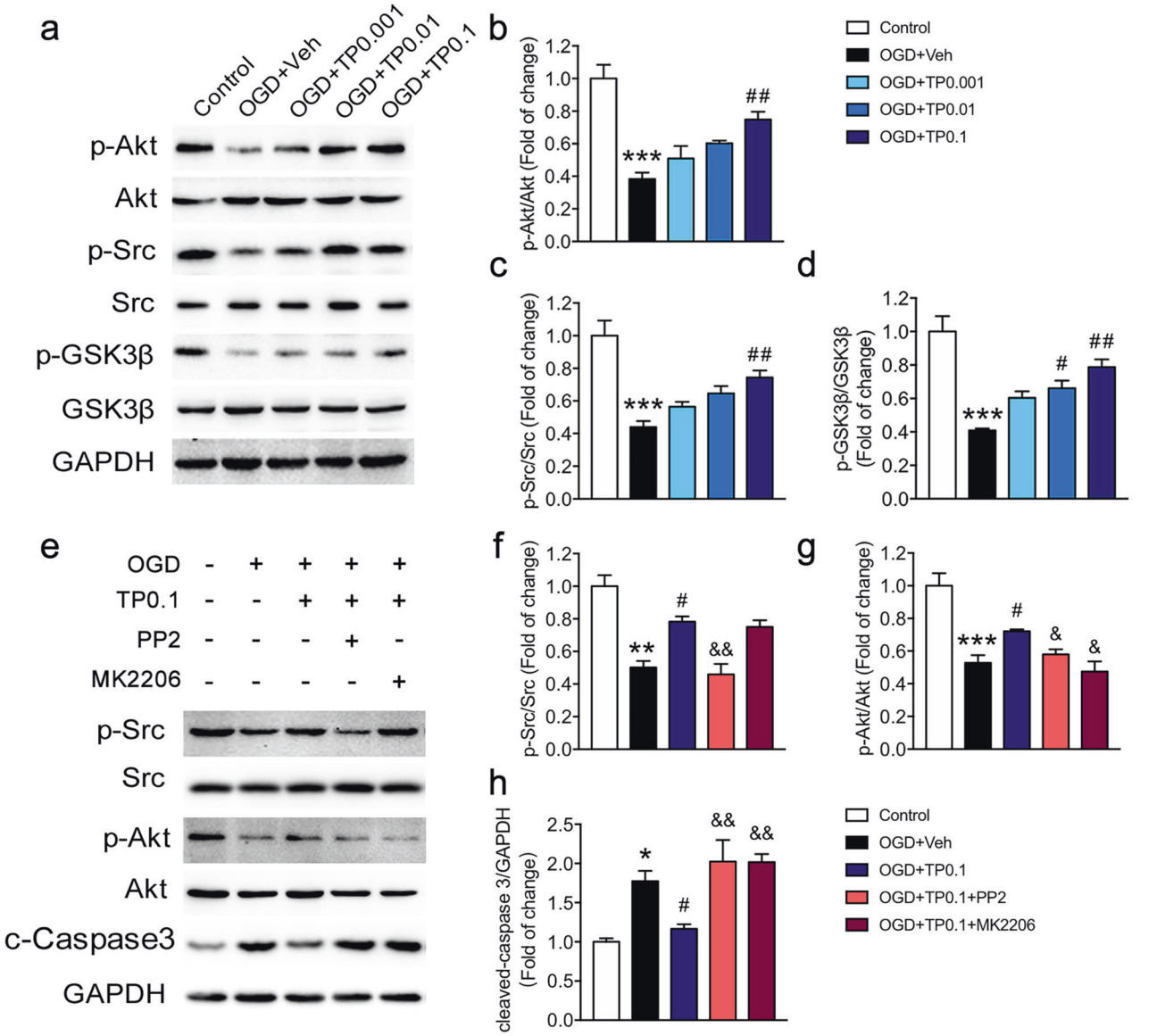

Fig. 4 Triptolide regulated the OGD-induced apoptosis of oligodendrocytes through the Src/Akt/GSK-3β signaling pathway. a–d Western blot analysis of p-Src, Src, p-Akt, Akt, p-GSK-3β, and GSK-3β expression in oligodendrocytes subjected to OGD for 2 h and administered with triptolide (0.001, 0.01, and 0.1 nM) for 1 h during reperfusion. **e–g** Western blot analysis of p-Src, Src, p-Akt, and Akt expression in oligodendrocytes subjected to OGD and treated with the Src inhibitor PP2 or the Akt inhibitor MK2206 followed by triptolide (0.1 nM). **e**, **h** Western blot analysis of cleaved-Caspase-3 (c-Caspase-3) expression in oligodendrocytes subjected to OGD and treated with the Src inhibitor PP2 or the Akt inhibitor MK2206 followed by triptolide (0.1 nM). $n = 3$–4 from at least three independent experiments. $^{*}P < 0.05$, $^{**}P < 0.01$, $^{***}P < 0.001$ vs. the control group; $^{\#}P < 0.05$, $^{\#\#}P < 0.01$ vs. the OGD + Veh group; $^{\&}P < 0.05$, $^{\&\&}P < 0.01$ vs. the OGD + TP0.1 group.

the level of phospho-Akt induced by triptolide treatment following OGD (Fig. 4e–g). Both PP2 and MK2206 blocked the downregulation of cleaved-Caspase-3 in oligodendrocytes treated with triptolide after OGD (Fig. 4e, h). All these data indicated that triptolide suppressed oligodendrocyte apoptosis by activating the Src/Akt/GSK3β signaling pathway.

Triptolide suppressed microglial activation and the expression of proinflammatory cytokines after chronic cerebral hypoperfusion

Microglial activation seems to be an early indicator of subsequent white matter injury after chronic cerebral hypoperfusion [33, 34]. Hyperactive microglia further exacerbate white matter injury and neuronal damage via proinflammatory effects [35]. It has been reported that microglial activation induced by lipopolysaccharide (LPS) was inhibited by triptolide treatment [12–14]. We thus studied the effect of triptolide on microglial activation by characterizing the morphology of Iba-1^{+} microglia and measuring the production of proinflammatory cytokines after rUCCAO or OGD using ELISAs. The results showed that rUCCAO induced an enlarged area of Iba-1^{+} microglia and increased TNF-α and IL-6 expression in the white matter, and these alterations were reduced by triptolide treatment at a dosage of 20 μg·kg^{-1}·d^{-1} (Fig. 5a–d). We also investigated the expression of proinflammatory cytokines in BV2 cells exposed to OGD for 2 h. TNF-α and IL-6 expression was increased in OGD-treated BV2 cells, but this effect was reduced by triptolide in a dose-dependent manner (Fig. 5e, f). The results indicated that triptolide suppressed microglial activation and proinflammatory cytokine expression after chronic cerebral hypoperfusion.

To investigate the role of neuroinflammation inhibition in the protective effect of triptolide against white matter injury, primary

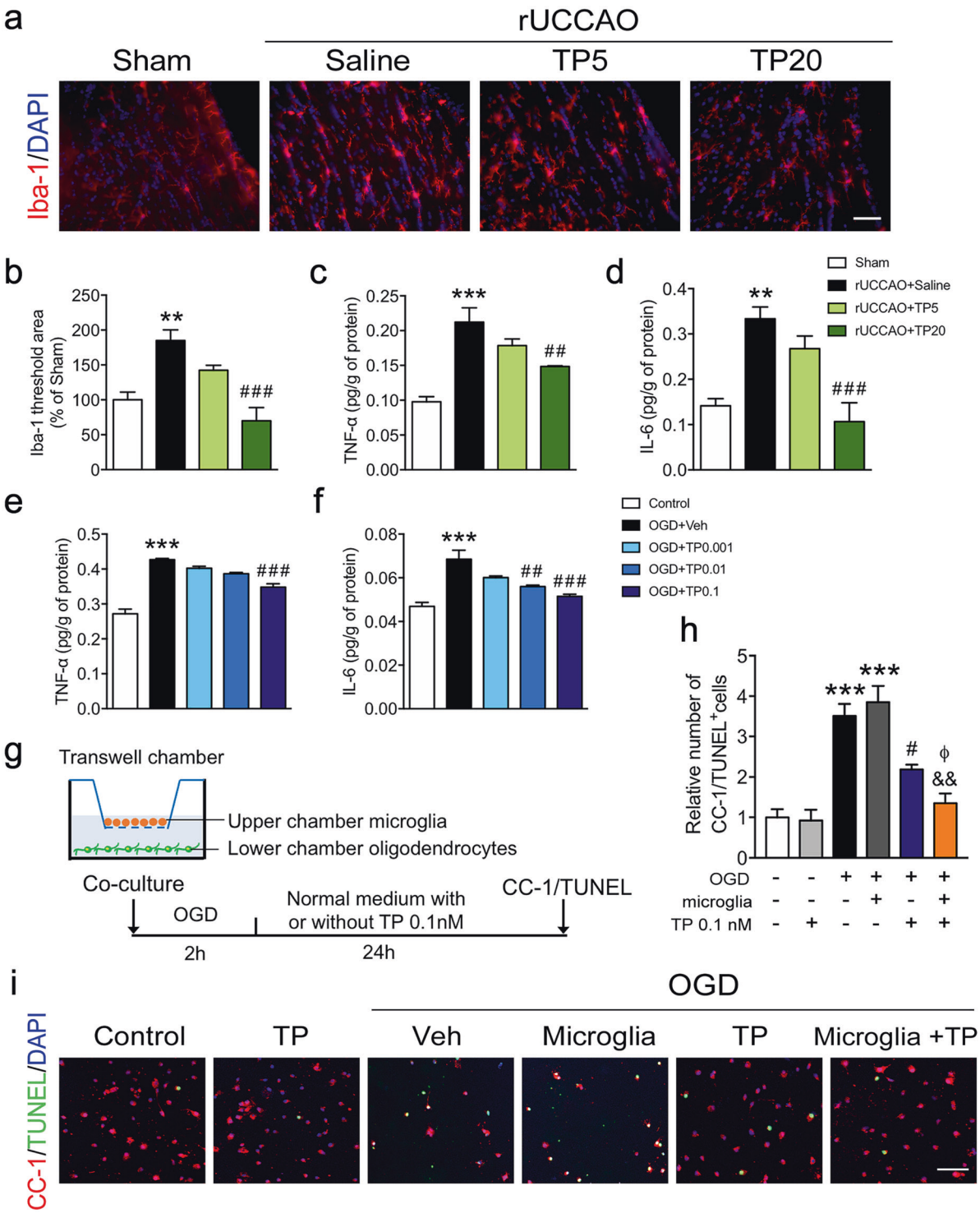

Fig. 5 Triptolide suppressed microglial activation and the expression of proinflammatory cytokines after chronic cerebral hypoperfusion or OGD. a, **b** Immunohistochemical visualization, morphological characterization, and quantification of Iba-1^{+} microglia at 7 d after rUCCAO in mice administered with triptolide at dosage of 5 μg·kg^{-1}·d^{-1} (TP5) or 20 μg·kg^{-1}·d^{-1} (TP20). **c**, **d** ELISA of TNF-α and IL-6 levels in the corpus callosum at 7 d after rUCCAO in mice administered with TP5 or TP20. **e**, **f** ELISA of TNF-α and IL-6 levels in BV2 cells subjected to OGD for 2 h and administered with triptolide (0.001, 0.01, and 0.1 nM) for 1 h during reperfusion. **g** Schematic diagram of coculture experiments using a Transwell system. Primary cultured oligodendrocytes and microglia were isolated by the shake-off method from mixed cortical glial cell cultures. Microglia were cocultured with mature oligodendrocytes in a Transwell system and subsequently subjected to OGD for 2 h and treated with or without triptolide (0.1 nM) for 24 h during reperfusion. **h**, **i** Immunohistochemical visualization and quantification of the numbers of CC-1 and TUNEL double-positive mature apoptotic oligodendrocytes after OGD/reperfusion. Scale bars, 50 μm. $n = 4$–5 from at least three independent experiments. $^{**}P < 0.01$, $^{***}P < 0.001$ vs. the sham group or the control group; $^{\#}P < 0.05$, $^{\#\#}P < 0.01$, $^{\#\#\#}P < 0.001$ vs. the rUCCAO + saline group or the OGD + Veh group; $^{\&\&}P < 0.01$ vs. the OGD + microglia group; $^{\Phi}P < 0.05$ vs. the OGD + TP 0.1 group.

oligodendrocytes and microglia were cocultured in a Transwell system, subjected to OGD for 2 h and treated with triptolide 0.1 nM for 24 h during reperfusion. The results showed that the number of CC-1 and TUNEL double-positive apoptotic oligodendrocytes was increased after OGD/reperfusion in both the coculture and monoculture systems, whereas treatment with triptolide significantly inhibited cell apoptosis. Notably, oligodendrocyte apoptosis after triptolide treatment in the coculture system was lower than that in the monoculture system (Fig. 5g–i). The results suggested that the inhibition of microglial inflammation by triptolide may also contribute to its alleviation of oligodendrocyte damage. In addition, 0.1 nM triptolide had no effect on the apoptosis of primary cultured oligodendrocytes without OGD exposure (Fig. 5h, i).

Treatment with triptolide at 20 μg·kg^{-1}·d^{-1} after chronic cerebral hypoperfusion had no hepatotoxic or nephrotoxic effects

Hepatotoxicity and nephrotoxicity are common complications of triptolide treatment. To investigate the toxicity in the liver and kidney resulting from triptolide treatment at 20 μg·kg^{-1}·d^{-1} for 28 days after chronic cerebral hypoperfusion, we evaluated liver function by testing the levels of alanine aminotransferase (ALT) and aspartate aminotransferase (AST) and assessed kidney function by measuring the levels of total albumin (ALB), blood urea nitrogen (BUN) and creatinine in serum after rUCCAO. The results showed that there were no differences in these serum biochemical indicators among all the groups. Thus, chronic triptolide treatment at 20 μg·kg^{-1}·d^{-1} after chronic cerebral hypoperfusion had no hepatotoxic or nephrotoxic effects.

DISCUSSION

This is the first study to reveal that triptolide alleviated oligodendrocyte loss to prevent white matter injury, including demyelination and axonal injury, and improved cognitive impairment following chronic cerebral hypoperfusion. We found that triptolide treatment inhibited oligodendrocyte apoptosis through the Src/Akt/GSK3β pathway and suppressed microglial activation in both in vivo and in vitro experiments. In addition, the low dosage of triptolide (20 μg·kg^{-1}·d^{-1}) did not show apparent hepatotoxicity or nephrotoxicity. Thus, triptolide may have potential applications in the clinic to treat conditions induced by chronic cerebral hypoperfusion, such as SIVD.

Triptolide is used as a drug to treat several white matter injury diseases, such as multiple sclerosis and experimental autoimmune encephalomyelitis (EAE), by inhibiting the activation of inflammatory cells and the secretion of proinflammatory mediators. Interestingly, we found that triptolide alleviated oligodendrocyte loss (Fig. 1) and directly reduced oligodendrocyte apoptosis (Supplementary Fig. 3a) after chronic cerebral hypoperfusion. Our results also showed concentration-dependent protective effects in mature oligodendrocytes exposed to OGD (Fig. 3a, b). Treatment with triptolide decreased mature oligodendrocyte apoptosis and the expression of the proapoptotic protein Bax and cleaved-Caspase 3 following OGD (Fig. 3e–i). Although triptolide was recently reported to improve cognitive dysfunction in rats with vascular dementia [20], its effects on white matter and oligodendrocytes have not been studied. We found that treatment with triptolide significantly reduced myelin and axon injury in both the corpus callosum and the hippocampus (Fig. 1a–d). Our findings indicated that triptolide can directly suppress oligodendrocyte apoptosis to alleviate white matter injury to relieve cognitive impairments after chronic cerebral hypoperfusion.

It has been reported that triptolide affects tumor cell proliferation and apoptosis by regulating the MAPK signaling pathway [27, 28, 36]. However, treatment with triptolide had no effect on the elevated expression of phosphorylated MAPKs, including phospho-ERK1/2, phospho-JNK and phospho-p38, in oligodendrocytes after OGD (Supplementary Fig. 2). In addition, previous studies have reported that high doses of triptolide (30–1000 nM) induced apoptosis via downregulation of the Akt signaling pathways in tumor cells [28, 37]. We found that low doses of triptolide (0.001–0.1 nM) exerted antiapoptotic effects by upregulating phospho-Akt during OGD in oligodendrocytes (Fig. 4a, b). Therefore, we hypothesized that

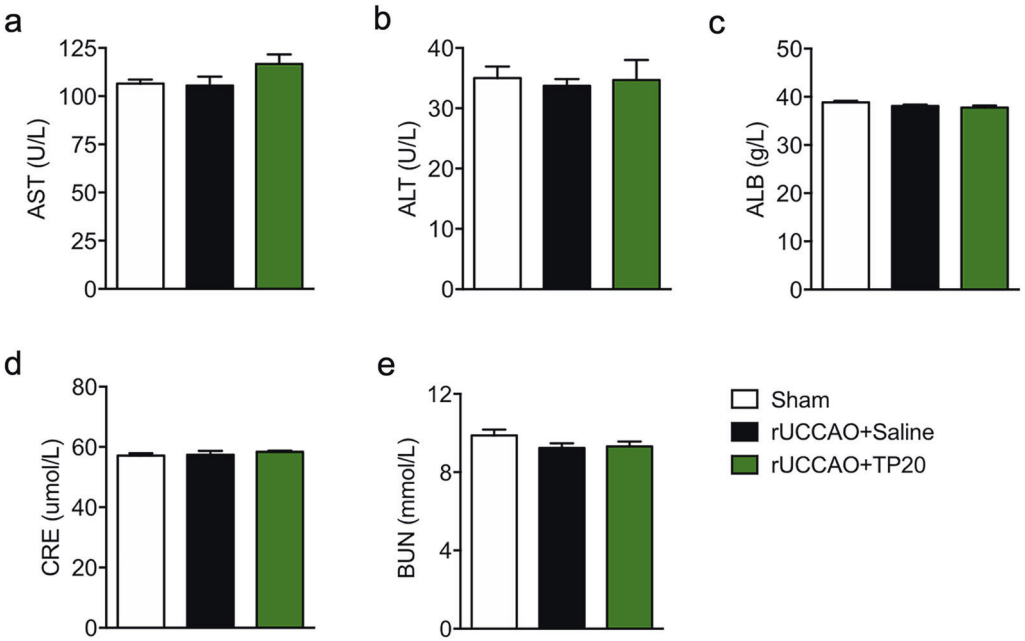

Fig. 6 Treatment with triptolide at 20 μg·kg^{-1}·d^{-1} after chronic cerebral hypoperfusion had no hepatotoxic or nephrotoxic effects. Liver function was evaluated by measuring the levels of (**a**) aspartate aminotransferase (AST) and (**b**) alanine aminotransferase (ALT), and kidney function was evaluated by measuring the levels of (**c**) total albumin (ALB), (**d**) creatinine and (**e**) blood urea nitrogen (BUN) in serum at 28 d after rUCCAO in mice administered with triptolide at a dosage of 20 μg·kg^{-1}·d^{-1} (TP20). $n = 6–7$ mice per group from at least three independent behavior experiments.

triptolide may exert dual effects on apoptosis depending upon its dose. It has been reported that triptolide induces apoptosis by inhibiting activation of Src in multiple myeloma cells [38]. Furthermore, many studies suggest that the Src/Akt/GSK3β signaling pathway is involved in the apoptosis of oligodendrocytes or Schwann cells [30–32]. The Src inhibitor PP2 suppresses the morphological differentiation of oligodendrocytes [39] and reduces the number of mature oligodendrocytes [40]. We demonstrated that treatment with low doses of triptolide elevated the phosphorylation of Src/Akt/GSK3β after rUCCAO (Supplementary Fig. 3b–d) or OGD (Fig. 4a–d), and these effects were abolished by the Src inhibitor PP2 or the Akt inhibitor MK2206 (Fig. 4e–g). Moreover, both PP2 and MK2206 blocked the downregulation of cleaved-Caspase-3 in oligodendrocytes treated with triptolide after OGD (Fig. 4e, h). All these data indicated that triptolide directly inhibited apoptosis by increasing the phosphorylation of the Src/Akt/GSK3β signaling pathway in vivo and in vitro.

In addition, microglial activation also plays a detrimental role in white matter injury following chronic cerebral hypoperfusion [33, 34]. Hyperactive microglia release a variety of cytotoxic mediators, including chemokines, proinflammatory cytokines, arachidonic acid derivatives, and reactive oxygen intermediates. Triptolide was shown to inhibit microglial activation and reduce the secretion of TNF-α and IL-1β in microglial cultures in a dose-dependent manner [14]. In the present study, we found that triptolide suppressed microglial activation and TNF-α and IL-6 expression in mice after chronic cerebral hypoperfusion and in cultured cells in vitro (Fig. 5a–f). In addition, the loss of oligodendrocytes can be alleviated by reducing microglia-mediated neuroinflammation after white matter damage caused by cerebral hypoperfusion [41]. We employed a Transwell coculture system and found that oligodendrocyte apoptosis after triptolide treatment in the coculture system was lower than that in the monoculture system (Fig. 5g–i). Taken together, these results suggested that triptolide alleviated white matter injury induced by chronic cerebral hypoperfusion directly by preventing oligodendrocyte apoptosis and indirectly by inhibiting microglial inflammation. This mechanism is different from that in ischemic stroke, in which triptolide protected neurons by inhibiting inflammation via the NF-κB signaling pathway [42, 43], restoring autophagy [44], or inhibiting apoptosis by activating the PI3K/Akt/mTOR pathway and inactivating the ERK1/2 pathway [45].

Although triptolide has been applied to treat rheumatism and immune diseases in the clinic and shows many pharmacological effects in vivo and in vitro, its applications have been restricted due to its multitarget toxicity, including reproductive toxicity, hepatotoxicity and nephrotoxicity. An increasing number of studies have demonstrated that triptolide-induced toxicity depends on the dosage and duration of treatment. For example, in vitro treatment with triptolide at 5–20 nM for 24 h inhibited the production of estradiol in rat granulosa cells [46]. Treatment with triptolide at 2.5–10 μM for 24 h induced mitochondrial impairment in isolated rat liver mitochondria and a normal human liver cell line [47]. In vivo administration of triptolide at 500 μg/kg for 24 h increased ALT and AST levels in the serum of mice [48]. Administration of triptolide at 200–400 $\mu g \cdot kg^{-1} \cdot d^{-1}$ for 28 d induced liver injury by inhibiting the mitochondrial respiratory chain [49]. In addition, rats administered with triptolide at 100–400 $\mu g \cdot kg^{-1} \cdot d^{-1}$ for 28 d exhibited nephrotoxicity, and the toxicity targeted the proximal tubule [50]. In our study, the neuroprotective effects of triptolide were present at much lower doses than those in previous studies [7–9, 12], that is, at 20 $\mu g \cdot kg^{-1} \cdot d^{-1}$ in vivo and 0.1 nM in vitro. Importantly, mice administered with triptolide at 20 $\mu g \cdot kg^{-1} \cdot d^{-1}$ did not show hepatotoxicity or nephrotoxicity even after 28 d of treatment (Fig. 6). Therefore, the low dosage of triptolide has potential clinical application value for the treatment of SIVD induced by chronic cerebral hypoperfusion.

In conclusion, the present investigation indicated that triptolide alleviated white matter injury induced by chronic cerebral hypoperfusion directly by preventing oligodendrocyte apoptosis via regulation of the Src/Akt/GSK3β pathway and indirectly by inhibiting microglial inflammation. The findings of this study indicate that triptolide is a promising treatment for SIVD induced by chronic cerebral hypoperfusion.

ACKNOWLEDGEMENTS

This work was supported by the Zhejiang Provincial Natural Science Foundation of China under Grants No. LR17H310001, and the National Natural Science Foundation of China (81803502, 81722045), and the Fundamental Research Funds for the Central Universities.

AUTHOR CONTRIBUTIONS

LJ and WWH designed the study and wrote the manuscript; YSW, YY, and QYD performed most of the experiments; YXX carried out most of the behavior experiments; HC, RRW, and YWH contributed to organizing the results; ZC, WWH, and LJ edited the manuscript. All authors reviewed and approved the manuscript.

Compliance with ethical standards

ADDITIONAL INFORMATION

Supplementary information The online version contains supplementary material available at https://doi.org/10.1038/s41401-021-00637-0.

Conflict of interest: The authors declare no competing interests.

REFERENCES

1. Selnes OA, Vinters HV. Vascular cognitive impairment. Nat Clin Pract Neurol. 2006;2:538–47.
2. Noel P, Von Hoff DD, Saluja AK, Velagapudi M, Borazanci E, Han H. Triptolide and its derivatives as cancer therapies. Trends Pharmacol Sci. 2019;40:327–41.
3. Yuan K, Li X, Lu Q, Zhu Q, Jiang H, Wang T, et al. Application and mechanisms of triptolide in the treatment of inflammatory diseases-a review. Front Pharmacol. 2019;10:1469.
4. Xi C, Peng S, Wu Z, Zhou Q, Zhou J. Toxicity of triptolide and the molecular mechanisms involved. Biomed Pharmacother. 2017;90:531–41.
5. Li XJ, Jiang ZZ, Zhang LY. Triptolide: progress on research in pharmacodynamics and toxicology. J Ethnopharmacol. 2014;155:67–79.
6. Zheng Y, Zhang WJ, Wang XM. Triptolide with potential medicinal value for diseases of the central nervous system. CNS Neurosci Ther. 2013;19:76–82.
7. Wu C, Xia Y, Wang P, Lu L, Zhang F. Triptolide protects mice from ischemia/reperfusion injury by inhibition of IL-17 production. Int Immunol Pharmacol. 2011;11:1564–72.
8. Lee HF, Lee TS, Kou YR. Anti-inflammatory and neuroprotective effects of triptolide on traumatic brain injury in rats. Respir Physiol Neurobiol. 2012;182:1–8.
9. Wang W, Mei XP, Chen L, Tang J, Li JL, Wu SX, et al. Triptolide prevents and attenuates neuropathic pain via inhibiting central immune response. Pain Phys. 2012;15:E995–1006.
10. Hu JY, Li CL, Wang YW. Intrathecal administration of triptolide, a T lymphocyte inhibitor, attenuates chronic constriction injury-induced neuropathic pain in rats. Brain Res. 2012;1436:122–9.
11. Wang X, Liang XB, Li FQ, Zhou HF, Liu XY, Wang JJ, et al. Therapeutic strategies for Parkinson's disease: the ancient meets the future–traditional Chinese herbal medicine, electroacupuncture, gene therapy and stem cells. Neurochem Res. 2008;33:1956–63.
12. Huang Y, Zhu N, Chen T, Chen W, Kong J, Zheng W, et al. Triptolide suppressed the microglia activation to improve spinal cord injury through miR-96/IKKbeta/NF-kappaB pathway. Spine (Philos Pa 1976). 2019;44:E707–E14.
13. Huang YY, Zhang Q, Zhang JN, Zhang YN, Gu L, Yang HM, et al. Triptolide up-regulates metabotropic glutamate receptor 5 to inhibit microglia activation in the lipopolysaccharide-induced model of Parkinson's disease. Brain Behav Immun. 2018;71:93–107.
14. Zhou HF, Niu DB, Xue B, Li FQ, Liu XY, He QH, et al. Triptolide inhibits TNF-alpha, IL-1 beta and NO production in primary microglial cultures. Neuroreport. 2003;14:1091–5.

15. Jiao J, Xue B, Zhang L, Gong Y, Li K, Wang H, et al. Triptolide inhibits amyloid-beta1-42-induced TNF-alpha and IL-1beta production in cultured rat microglia. J Neuroimmunol. 2008;205:32–6.
16. Ma J, Xiong JY, Hou WW, Yan HJ, Sun Y, Huang SW, et al. Protective effect of carnosine on subcortical ischemic vascular dementia in mice. CNS Neurosci Ther. 2012;18:745–53.
17. Youssef MI, Zhou Y, Eissa IH, Wang Y, Zhang J, Jiang L, et al. Tetradecyl 2,3-dihydroxybenzoate alleviates oligodendrocyte damage following chronic cerebral hypoperfusion through IGF-1 receptor. Neurochem Int. 2020;138:104749.
18. Yoshizaki K, Adachi K, Kataoka S, Watanabe A, Tabira T, Takahashi K, et al. Chronic cerebral hypoperfusion induced by right unilateral common carotid artery occlusion causes delayed white matter lesions and cognitive impairment in adult mice. Exp Neurol. 2008;210:585–91.
19. Zhou Y, Zhang J, Wang L, Chen Y, Wan Y, He Y, et al. Interleukin-1beta impedes oligodendrocyte progenitor cell recruitment and white matter repair following chronic cerebral hypoperfusion. Brain Behav Immun. 2017;60:93–105.
20. Yao P, Li Y, Yang Y, Yu S, Chen Y. Triptolide improves cognitive dysfunction in rats with vascular dementia by activating the SIRT1/PGC-1alpha signaling pathway. Neurochem Res. 2019;44:1977–85.
21. Sanadgol N, Golab F, Mostafaie A, Mehdizadeh M, Khalseh R, Mahmoudi M, et al. Low, but not high, dose triptolide controls neuroinflammation and improves behavioral deficits in toxic model of multiple sclerosis by dampening of NF-kappaB activation and acceleration of intrinsic myelin repair. Toxicol Appl Pharmacol. 2018;342:86–98.
22. Wang Y, Mei Y, Feng D, Xu L. Triptolide modulates T-cell inflammatory responses and ameliorates experimental autoimmune encephalomyelitis. J Neurosci Res. 2008;86:2441–9.
23. Shi Y, Shao Q, Li Z, Gonzalez GA, Lu F, Wang D, et al. Myt1L promotes differentiation of oligodendrocyte precursor cells and is necessary for remyelination after lysolecithin-induced demyelination. Neurosci Bull. 2018;34:247–60.
24. Yu SY, Zhang XY, Wang XR, Xu DM, Chen L, Zhang LH, et al. Cysteinyl leukotriene receptor 1 mediates LTD4-induced activation of mouse microglial cells in vitro. Acta Pharmacol Sin. 2014;35:33–40.
25. Herrera MI, Udovin LD, Toro-Urrego N, Kusnier CF, Luaces JP, Otero-Losada M, et al. Neuroprotection targeting protein misfolding on chronic cerebral hypoperfusion in the context of metabolic syndrome. Front Neurosci. 2018;12:339.
26. Fang YC, Chan L, Liou JP, Tu YK, Lai MJ, Chen CI, et al. HDAC inhibitor protects chronic cerebral hypoperfusion and oxygen-glucose deprivation injuries via H3K14 and H4K5 acetylation-mediated BDNF expression. J Cell Mol Med. 2020;24:6966–77.
27. Yanchun M, Yi W, Lu W, Yu Q, Jian Y, Pengzhou K, et al. Triptolide prevents proliferation and migration of esophageal squamous cell cancer via MAPK/ERK signaling pathway. Eur J Pharmacol. 2019;851:43–51.
28. Tan BJ, Chiu GN. Role of oxidative stress, endoplasmic reticulum stress and ERK activation in triptolide-induced apoptosis. Int J Oncol. 2013;42:1605–12.
29. Wang M, Chen B, Chai L. Triptolide suppresses the proliferation and induces the apoptosis of nasopharyngeal carcinoma cells via the PI3K/Akt pathway. Oncol Lett. 2019;17:1372–8.
30. Cui QL, Zheng WH, Quirion R, Almazan G. Inhibition of Src-like kinases reveals Akt-dependent and -independent pathways in insulin-like growth factor I-mediated oligodendrocyte progenitor survival. J Biol Chem. 2005;280:8918–28.
31. Cui QL, Fogle E, Almazan G. Muscarinic acetylcholine receptors mediate oligodendrocyte progenitor survival through Src-like tyrosine kinases and PI3K/Akt pathways. Neurochem Int. 2006;48:383–93.
32. Li R, Wu Y, Zou S, Wang X, Li Y, Xu K, et al. NGF attenuates high glucose-induced ER stress, preventing schwann cell apoptosis by activating the PI3K/Akt/GSK3beta and ERK1/2 pathways. Neurochem Res. 2017;42:3005–18.
33. Wakita H, Tomimoto H, Akiguchi I, Kimura J. Glial activation and white matter changes in the rat brain induced by chronic cerebral hypoperfusion: an immunohistochemical study. Acta Neuropathol. 1994;87:484–92.
34. Farkas E, Donka G, de Vos RA, Mihaly A, Bari F, Luiten PG. Experimental cerebral hypoperfusion induces white matter injury and microglial activation in the rat brain. Acta Neuropathol. 2004;108:57–64.
35. Huang J, Liu G, Shi B, Shi G, He X, Lu Z, et al. Inhibition of microglial activation by minocycline reduced preoligodendrocyte injury in a neonatal rat brain slice model. J Thorac Cardiovasc Surg. 2018;156:2271–80.
36. Qin W, Li S, Miao Y, Shi Q, Wang Y, Li J, et al. Triptolide induces mitochondrial apoptosis through modulating dual specificity phosphatase 1/mitogen-activated protein kinases cascade in osteosarcoma cells. Neoplasma. 2018;65:21–33.
37. Liu X, Zhao P, Wang X, Wang L, Zhu Y, Gao W, et al. Triptolide induces glioma cell autophagy and apoptosis via upregulating the ROS/JNK and downregulating the Akt/mTOR signaling pathways. Front Oncol. 2019;9:387.
38. Kim JH, Park B. Triptolide blocks the STAT3 signaling pathway through induction of protein tyrosine phosphatase SHP-1 in multiple myeloma cells. Int J Mol Med. 2017;40:1566–72.
39. Osterhout DJ, Wolven A, Wolf RM, Resh MD, Chao MV. Morphological differentiation of oligodendrocytes requires activation of Fyn tyrosine kinase. J Cell Biol. 1999;145:1209–18.
40. Sperber BR, McMorris FA. Fyn tyrosine kinase regulates oligodendroglial cell development but is not required for morphological differentiation of oligodendrocytes. J Neurosci Res. 2001;63:303–12.
41. Qin C, Zhou LQ, Ma XT, Hu ZW, Yang S, Chen M, et al. Dual functions of microglia in ischemic Stroke. Neurosci Bull. 2019;35:921–33.
42. Yang B, Yan P, Yang GZ, Cao HL, Wang F, Li B. Triptolide reduces ischemia/reperfusion injury in rats and H9C2 cells via inhibition of NFkappaB, ROS and the ERK1/2 pathway. Int J Mol Med. 2018;41:3127–36.
43. Hao M, Li X, Feng J, Pan N. Triptolide protects against ischemic stroke in rats. Inflammation. 2015;38:1617–23.
44. Yang Y, Gao K, Hu Z, Li W, Davies H, Ling S, et al. Autophagy upregulation and apoptosis downregulation in DAHP and triptolide treated cerebral ischemia. Mediators Inflamm. 2015;2015:120198.
45. Li W, Yang Y, Hu Z, Ling S, Fang M. Neuroprotective effects of DAHP and triptolide in focal cerebral ischemia via apoptosis inhibition and PI3K/Akt/mTOR pathway activation. Front Neuroanat. 2015;9:48.
46. Zhang J, Liu L, Mu X, Jiang Z, Zhang L. Effect of triptolide on estradiol release from cultured rat granulosa cells. Endocr J. 2012;59:473–81.
47. Fu Q, Jiang ZZ, Zhang LY. Impairment of triptolide on liver mitochondria in isolated liver mitochondria and HL7702 cell line. Chin J Integr Med. 2013;19:683–8.
48. Wang X, Jiang Z, Cao W, Yuan Z, Sun L, Zhang L. Th17/Treg imbalance in triptolide-induced liver injury. Fitoterapia. 2014;93:245–51.
49. Fu Q, Huang X, Shu B, Xue M, Zhang P, Wang T, et al. Inhibition of mitochondrial respiratory chain is involved in triptolide-induced liver injury. Fitoterapia. 2011;82:1241–8.
50. Sun L, Li H, Huang X, Wang T, Zhang S, Yang J, et al. Triptolide alters barrier function in renal proximal tubular cells in rats. Toxicol Lett. 2013;223:96–102.